

ARTICLE

Characteristics and Significance of Carbon and Oxygen Isotopic Compositions of the PTB Boundary in Haidai Section, Xuanwei Area of China

Chenming Liu ¹, Demin Yang ^{1*}, Zhengqin Na ²

¹Institute of Resources and Environment, Yunnan Land and Resources Vocational College, Kunming 650093, China

²Yunnan Wuyuan Technology Co., Ltd., Kunming 650027, China

ABSTRACT

The End-Permian mass extinction (EPME), Earth's most severe biocrisis, occurred proximal to the Permian-Triassic Boundary (PTB), with marine ecosystems experiencing catastrophic collapse. This study employs stable carbon ($\delta^{13}\text{C}$) and oxygen isotopes from marine carbonates in the Haidai Section (Xuanwei, northeastern Yunnan) to decipher paleoenvironmental drivers. The well-preserved stratigraphic sequence encompasses the Upper Permian (Yangxin and Xuanwei Formations) transitioning into the Lower Triassic (Feixianguan and Jialingjiang Formations), providing a continuous marine sedimentary archive. A marked negative $\delta^{13}\text{C}$ excursion (-9.66% V-PDB) occurs at the PTB, initiating from $+0.82\%$ with subsequent gradual recovery. This geochemical signature correlates with: 90% reduction in primary productivity Biodiversity collapse exhibiting cluster extinction patterns Prolonged suppression of ecological recovery Concurrently, reconstructed seawater temperatures reveal extreme thermal fluctuations, surging from $23\text{ }^{\circ}\text{C}$ to $32\text{ }^{\circ}\text{C}$ at the PTB before precipitously declining to $16\text{ }^{\circ}\text{C}$. These perturbations demonstrate coupled biogeochemical dynamics wherein: • Carbon cycle destabilization disrupted nutrient fluxes. • Temperature oscillations exceeded marine taxa thermal tolerances. • Synergistic environmental stresses amplified extinction selectivity. The $\delta^{13}\text{C}$ -temperature covariance ($r^2 = 0.085$) establishes mechanistic linkages between physicochemical perturbations and biotic responses. Our findings demonstrate that the EPME was driven by positive feedback loops in which: Volcanic CO_2 emissions triggered carbonate saturation decline Thermal

*CORRESPONDING AUTHOR:

Demin Yang, Institute of Resources and Environment, Yunnan Land and Resources Vocational College, Kunming 650093, China; Email: 28924210@qq.com

ARTICLE INFO

Received: 20 January 2025 | Revised: 26 February 2025 | Accepted: 5 March 2025 | Published Online: 6 May 2025

DOI: <https://doi.org/10.30564/jees.v7i5.8500>

CITATION

Liu, C, Yang, D., Na, Z., 2025. Characteristics and Significance of Carbon and Oxygen Isotopic Compositions of the PTB Boundary in Haidai Section, Xuanwei Area of China. *Journal of Environmental & Earth Sciences*. 7(5): 203–214. DOI: <https://doi.org/10.30564/jees.v7i5.8500>

COPYRIGHT

Copyright © 2025 by the author(s). Published by Bilingual Publishing Group. This is an open access article under the Creative Commons Attribution-NonCommercial 4.0 International (CC BY-NC 4.0) License (<https://creativecommons.org/licenses/by-nc/4.0/>).

stratification exacerbated anoxia Biogeochemical cycling perturbations suppressed primary producers This integrated geochemical record from the Haidai Section provides critical insights into environment-organism coevolution during Phanerozoic Earth's most profound mass extinction.

Keywords: Carbon and Oxygen Isotope; Northeastern Yunnan; Xuanwei; PTB; ELIP; Mass Extinction

1. Introduction

The mass extinction event at the Permian-Triassic Boundary (PTB) stands as the most severe ecosystem collapse in the Phanerozoic, resulting in the extinction of approximately 90% of marine species and 70% of terrestrial vertebrates^[1–3]. This event is highly coupled with drastic changes in the global carbon cycle, ancient ocean anoxia, and extreme climate fluctuations, making carbon and oxygen isotope analysis a pivotal tool for unveiling its environmental driving mechanisms^[4]. Carbon isotopes ($\delta^{13}\text{C}$), serving as tracers of ancient carbon cycles, exhibit a widely recognized global negative excursion (about 3–8‰) that is a hallmark of the PTB^[5]. The mechanisms behind this excursion (such as mass extinction, massive methane hydrate release, and organic carbon oxidation triggered by Siberian Large Igneous Province activity) are directly linked to the surge in greenhouse gases and ocean acidification. Due to the geochemical behavior of photosynthesis in algae and other organisms, which selectively absorb carbon isotopes from the atmosphere, preferring ^{12}C for organic matter synthesis, this process leads to an enrichment of ^{13}C and depletion of ^{12}C in contemporaneously precipitated carbonate rocks, which is preserved in the rocks^[6, 7]. When algae and other organisms undergo mass extinction, the selective absorption of photosynthesis is significantly affected, leading to a relative increase in ^{12}C and depletion of ^{13}C in carbonate rocks. This process, recorded in contemporaneously precipitated carbonate rocks, provides an important reference for studying biological extinctions. Studies have shown that inorganic carbon isotopes ($\delta^{13}\text{C}$) near the P-T boundary commonly exhibit an anomalous decrease of 2‰–4‰^[8, 9]. Oxygen isotopes ($\delta^{18}\text{O}$), by recording ancient seawater temperatures and ice sheet dynamics, reveal a possible abrupt global temperature rise of 5–8 °C during the PTB^[10–18]. The synergistic effects of this thermal stress and anoxic environments have been proven to have a fatal threshold effect on marine organisms. In recent years, high-resolution carbon and oxygen isotope

stratigraphic studies have further revealed the staged characteristics of the PTB event: the sustained negative excursion of $\delta^{13}\text{C}$ and anomalous fluctuations of $\delta^{18}\text{O}$ in the late Permian are precisely correlated with the first phase of biological extinction (at the end of the Guadalupian)^[19]; whereas the continued isotope disturbances in the early Triassic may reflect the long-term delayed recovery of ecosystems. Notably, the coupled anomalies of carbon and oxygen isotopes not only exhibit global isochronism (such as in the Meishan section in South China and the Khuff Formation in Mesopotamia) but also show a significant positive correlation between the fluctuation amplitude and extinction intensity on a spatial scale^[20–27], providing crucial geochemical constraints for the hypothesis of “environmental catastrophe-driven extinction”. The Yangtze Platform in South China is a classic region for studying the PTB event, preserving the world's most complete continuous marine strata. Northeast Yunnan, located on the southwestern margin of the Yangtze Platform, records an abrupt environmental transition from shallow marine to deep-water basin settings in its late Permian to early Triassic carbonate platform, manifested by a sharp decline in calcium carbonate content, rapid negative excursion of $\delta^{13}\text{C}_{\text{carb}}$ (about 4–6‰), and a mirror-image relationship with the positive excursion of $\delta^{13}\text{C}_{\text{org}}$, indicating the disturbance of the carbon cycle by terrestrial organic matter input and sea-level rise^[28]. This region also experienced multiple episodes of biological extinction, such as the succession of Late Ordovician brachiopod fauna (EC fauna) that was synchronous with carbon and oxygen isotope fluctuations, revealing the phased impact of environmental pressures on ecosystems. The Zhenxiong section in northeast Yunnan preserves the succession sequence from the Hirnantia Fauna to the EC fauna near the PTB, with a significant spatiotemporal correlation between biodiversity changes and $\delta^{13}\text{C}$ negative excursion events, providing regional evidence for the hypothesis of “environmental catastrophe-driven extinction”. The upper Permian Yangxin and Xuanwei formations, as well as the lower Triassic Feixianguan and Jialingjiang formations, are

well-developed and relatively continuous marine sedimentary rock series in the Xuanwei region of northeast Yunnan. Based on regional geological survey work in the study area, it has been found that a complete and continuous stratigraphic sequence, including the Yangxin, Xuanwei, Feixianguan, and Jialingjiang formations, is exposed in Yueliangtian Village, Haidai Town, Xuanwei region (**Figure 1**). This study aims to elucidate the dynamic link between carbon cycle-climate system instability and biological extinction on the southwestern margin of the Yangtze Platform by systematically analyzing carbon and oxygen isotope records in sedimentary rocks near the PTB boundary using $\delta^{13}\text{C}_{\text{carb}}$ and $\delta^{18}\text{O}$ data. The study will focus on the synergistic effects of marine ecosystem disruption and volcanic-hydrothermal activities, providing new geochemical constraints for the “multifactor coupling-driven model” of the PTB mass extinction and new isotopic geochemical evidence for understanding the triggering mechanisms and ecological effects of mass extinction events.

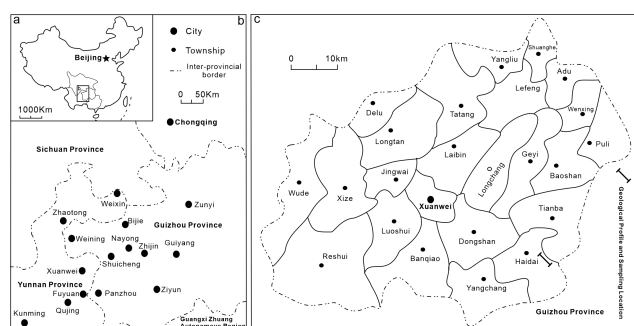


Figure 1. Sampling location map (modified^[29]): (a) and (b) the sampling location in Haidai Town, Xuanwei City, southwestern China's Yunnan Province; and (c) the research section located in Yueliangtian Village, Haidai Town, bordering on Guizhou Province. Note: The main stratigraphic sequence, from older to younger, includes the third member of the Middle Permian Yangxin Formation (P_{2y}^3), the Emeishan Basalt Formation (Pe), the Upper Permian Xuanwei Formation (P_{3x}), the Lower Triassic Feixianguan Formation (T_{1f}), and the Lower Triassic Jialingjiang Formation (T_{1j}). Continuous block sampling was conducted by stratigraphic layer, selecting unweathered samples, and a total of 46 original rock samples were collected.

2. Geological Background and Sample Collection

The study area belongs to the Upper Yangtze paleocontinental block, specifically the carbonate platform of eastern Yunnan, and the Qujing epicontinental sea^[29]. The sedimentary formations within the area mainly consist of the Upper Paleozoic to Mesozoic sequences. Among them, the Upper Devonian to the lower part of the Lower

Carboniferous are composed of platform carbonate formations. The middle to lower parts of the Lower Carboniferous are marine-continental transition facies coal-bearing argillaceous-siliceous formations. The middle part of the Lower Carboniferous to the Lower Permian are platform carbonate formations. The lower part of the Middle Permian is a marine-continental transition facies coal-bearing clastic formation, while the upper part is a platform carbonate formation. The Upper Permian consists of terrestrial volcanic rock formations and marine-continental transition facies coal-bearing clastic formations. The middle to lower parts of the Lower Triassic are composed of littoral to shallow marine shelf sandy-muddy carbonate formations. The upper part of the Lower Triassic to the lower part of the Middle Triassic are restricted platform carbonate formations. The middle part of the Middle Triassic is composed of shallow marine shelf sandy-muddy formations, while the upper part of the Middle Triassic to the lower part of the Upper Triassic are platform carbonate formations. The upper part of the Upper Triassic is composed of lacustrine clastic formations. The Lower Jurassic is composed of lacustrine clastic formations, the lower part of the Middle Jurassic is composed of lake delta glutenite formations, and the middle to upper parts of the Middle Jurassic are lacustrine clastic formations.

The Permian-Triassic boundary section is located in Yueliangtian Village, Haidai Town, Xuanwei City (**Figure 1**). The main stratigraphic sequence, from older to younger, includes the third member of the Yangxin Formation of the Middle Permian (P_{2y}^3), the Emeishan Basalt Formation (Pe), the Xuanwei Formation of the Upper Permian (P_{3x}), the Feixianguan Formation of the Lower Triassic (T_{1f}), and the Jialingjiang Formation of the Lower Triassic (T_{1j}). The rock strata are in conformable contact, and the boundary is well exposed and distinct. The lithological assemblage of the third member of the Yangxin Formation mainly consists of gray to dark gray medium- to thick-bedded micrite limestones and microcrystalline limestones, intercalated with a small amount of argillaceous limestones and siliceous banded limestones. The overall lithology of the Xuanwei Formation is a set of sandstone-mudstone interbeds with multiple coal seams. The lithological characteristics are mainly grayish yellow-green, gray-green thin to medium-thick bedded fine-grained lithic sandstones and feldspathic lithic sandstones, interspersed with grayish green, light purple-red, grayish white, gray, and

other variegated thin-bedded mudstones and argillaceous siltstones. Thin limestone lentils are occasionally intercalated within the rock formations. According to regional geological data, marine-terrestrial transitional deposits develop towards the east of the stratigraphic extension. The lithological characteristics of the Feixianguan Formation are grayish purple-red and light gray thin-bedded fine-grained lithic sandstones and feldspathic lithic sandstones, interspersed with dark purple-red thin-bedded argillaceous siltstones and silty mudstones, with multiple thin-bedded limestones. The lithological characteristics of the Jialingjiang Formation mainly consist of gray to grayish yellow thin to medium-bedded micrite limestones and worm-like limestones, with a touch of light purple-red. Carbonate rock samples were mainly collected from the section using a layered continuous block sampling method, selecting samples that were not weathered. Specific sampling horizons and locations are shown in **Figure 1**. The stratigraphic descriptions are as follows:

Yangxin Formation, Third Member (P_2y^3): The lithological association consists of gray, dark gray to grayish-black medium- to thick-bedded micrite limestones, microcrystalline limestones, siliceous banded dolomitic limestones, siliceous banded microcrystalline limestones, dolomitic bioclastic limestones, dolomites, fusulinid limestones, sandy limestones intercalated with argillaceous limestones, and bituminous argillaceous limestones, with an increase in dolomite content upwards. The fauna in this member mainly includes brachiopods, crinoid stems, fusulinids, and corals. Occasional horizontal laminations are observed in the limestones. A basic sequence is developed: gray thick-bedded massive microcrystalline limestone to bioclastic limestone. Fossils collected from this stratigraphic unit by previous researchers include *Nankinella* and *Sphaerulina* (fusulinids), *Liangshanophyllum cf. lipoense* (Huang) (coral), *Lino-productus sp.*, *Schizophoria sp.*, *Spiriferellina ornata var. orientalis* (Frech), and *Chonetes sp.* (brachiopods). The stratigraphic unit is dominated by thick-bedded massive limestones intercalated with multiple layers of dolomites. The rocks often contain intraclasts and silt clasts, and the middle to upper parts are intercalated with siliceous nodules, which commonly exhibit concentric structures, indicating a lateral infill origin. Horizontal bedding is developed in some rocks. The fossil assemblage is rich in marine benthic organisms, suggesting a depositional environment of an open carbonate

platform.

The Emeishan Basalt Formation (Pe): The lithological characteristics are mainly gray and light gray compact basalts and amygdaloidal basalts, intercalated with light purplish-red basaltic tuffs and tuffaceous mudstones, locally with porphyritic basalts. It is in eruptive unconformable contact with the underlying Yangxin Formation (P_2y^3) and is conformably overlain by the Upper Permian Xuanwei Formation (P_3x), with the limestone of the Yangxin Formation ending and the basalt starting as the stratigraphic exposure marker.

Upper Permian Xuanwei Formation (P_3x): The lithology generally consists of a suite of sandy-muddy rocks interbedded with multiple coal seams. The sedimentary grain size generally fines upwards. The lithological characteristics mainly include grayish-yellow-green, gray-green thin to locally medium-thick beds of fine-grained lithic sandstones, feldspathic lithic sandstones, and gray-green, light purplish-red, grayish-white, gray, and other variegated thin beds of mudstones (shales), silty mudstones (shales), argillaceous siltstones, and grayish-yellow iron-bearing mudstones, interspersed with occasional thin beds of limestone lenses, multiple thin to medium beds of black carbonaceous mudstones, and coal seams. Parallel bedding is developed in the sandstones, with occasional cross-bedding. Horizontal bedding is developed in the silt-mud rocks. Basic sequences include: A thin bed of fine-grained sandstone to shale; B thin bed of fine-grained sandstone to variegated mudstone (with unstable coal seams); C medium to thin beds of fine-grained sandstone to thin beds of silty mudstone, shale, and coal seam; D thin beds of silty mudstone to argillaceous siltstone rhythmic interbedding. Fossil plants include *Cigantopteris sp.*, *G. nicotianaefolia Schenk*, *G. lagrelii Halle*, *Pecopteris sp.*, *P. orientalis Halle*, *P. hemitelioides Brongniart*, *Asterphyllites pingloensis Sze*, *Protoblechnum wongii Halle*, *Lobatannularia heianensis* (Kodaira), *L. multifolia Konno et Asama*, *L. lingulata* (Halle), among others. The bottom of the formation consists of basaltic medium conglomerates intercalated with stratified and branching, unstable fine-grained lithic sandstones with parallel bedding, indicating fluvial (riverbed) depositional features. The middle part consists of medium to thin beds of fine sandstones interbedded with yellow-green variegated mudstones, iron-bearing mudstones, and multiple layers of carbonaceous mudstones or coal seams. Parallel bedding is developed in the sandstones, with occa-

sional cross-bedding. Horizontal bedding or laminations are developed in the silt-mud rocks. The depositional environment is dominated by swampy lacustrine deposits with intermittent exposure, leading to the development of poorly bedded iron-bearing mudstones. The top consists of yellow-green thin beds of silty mudstones with horizontal bedding, indicating shallow lacustrine deposition. The contact relationship between the Xuanwei Formation and the underlying Middle to Upper Permian Emeishan Basalt (Pe) varies regionally, with some areas showing parallel unconformable contact and others no contact. It is conformably overlain by the Lower Triassic Feixianguan Formation (T_{1f}).

The Feixianguan Formation of the Lower Triassic Series (T_{1f}): Based on lithological associations and rock colors, the Feixianguan Formation in the region can be divided into two members. The First Member of the Feixianguan Formation (T_{1f}^1): It mainly consists of a suite of purple-red clastic rocks. The lithological features include gray-purple-red and light gray thin-bedded fine-grained lithic sandstone, felsic lithic sandstone, and dark purple-red thin-bedded argillaceous siltstone and silty mudstone interbeds. The sandstones are characterized by parallel bedding, small oblique bedding, and large tabular cross-bedding, while the siltstone-mudstone develops horizontal bedding. Basic sequences developed include: A) dark purple-red fine-grained sandstone→light grayish purple fine-grained sandstone→dark purple-red argillaceous siltstone; B) thin-bedded fine-grained sandstone→thin-bedded argillaceous siltstone; C) thin-bedded fine-grained sandstone→thin-bedded (argillaceous) siltstone with sandstone interbeds; D) thin-bedded fine-grained sandstone→thin-bedded mudstone. The Second Member of the Feixianguan Formation (T_{1f}^2): Compared to the first member, the individual rock layers are thicker, and the rock colors are more varied. The lithological features include grayish yellow-green, light grayish purple medium-thin bedded silty mudstone, argillaceous silty shale, calcareous silty (shale) mudstone with grayish purple and yellowish green medium-thick bedded lithic sandstone and felsic lithic sandstone. In the middle and upper parts, thin-bedded light gray mudstone limestone develops, with an increase in carbonate components, reflecting a change in depositional environment from sandy-muddy to carbonate, indicating an increase in water depth. The sandstones are mostly characterized by parallel bedding, and the siltstone-mudstone mostly

develops horizontal bedding. Basic sequences developed include: A) medium-bedded fine-grained sandstone→thin-bedded fine-grained sandstone→silty mudstone interbeds; B) medium-thick bedded fine-grained sandstone→medium-thick bedded silty mudstone (shale); C) medium-thick bedded siltstone → medium-thick bedded silty mudstone (shale); D) medium-thin bedded fine-grained sandstone → argillaceous silty shale. Fossils collected by previous researchers include bivalves such as *Claraia griesbachi* (Bittner), *C. griesbachi var. cancentrica* (Yabe)?, *C. orbicularis* (Richthofen), *Oxytoma scythicum wirth*, etc.; brachiopods such as *Lingula tenuissima Bronn*, *L. ex gr. tenuissima Bronn*, etc.; ammonites such as *Lytophiceras? sp.*, *Ophiceras sp.*; ostracods such as *Euestheria? sp.*; and ammonites such as *Lytophiceras? sp.* The Feixianguan Formation is mainly a suite of littoral to shallow marine deposits. The first member is mainly composed of a suite of fine-grained sandstone with siltstone-mudstone interbeds. The sandstone grains are fine, belonging to the fine sand grain size, without medium to coarse sand or gravel, and are well-sorted. Worm burrows can be seen in the sandstones, with highly developed parallel bedding and large, medium, and small tabular cross-bedding. The bedding set angles are less than 25° , all being low-angle bedding, and ripple bedding can also be observed. The siltstone-mudstone has horizontal bedding and developed sandy laminae or lenticular bodies, representing foreshore to nearshore deposits. The second member consists of varicolored sandy-mudstone and sandstone interbeds with fine-grained and well-sorted sandstones. Parallel bedding can be seen in the sandstones, and horizontal bedding in the siltstone-mudstone, representing nearshore deposits. The upper to top parts are mainly composed of a suite of silty-mudstone shale, with calcium content at the top. The depositional grains are fine, with highly developed lamellar structures, representing shallow marine shelf silty-mudstone deposits. The Feixianguan Formation is in conformable contact with the underlying Xuanwei Formation of the Upper Permian Series (P_{3x}) and is conformably overlain by the Jialingjiang Formation of the Middle-Lower Triassic Series (T_{1j}).

Jialingjiang Formation (T_{1j}): The lithological features are mainly gray to grayish yellow with light purple-red medium-thin bedded mud-bearing micrite limestone and worm-like limestone interbeds. The limestones have well-

developed horizontal laminae and a basic sequence: gray and yellow-gray medium-thin bedded mud-bearing limestone → worm-like limestone. Fossils collected by previous researchers include bivalves such as *Eumorphotis sp.*, *Entolium discites microtis* (Bittner); gastropods such as *Naticopsis sp.*, *Loxonema sp.*, *Mentzelia sp.*, *Lingula cf. tenuissima Bronn*; ammonites such as *Tirolites spinosus Mojsisovics*, *Meekoceras latirentrosum Chao*, etc. The Jialingjiang Formation is mainly composed of a suite of medium-thin bedded mud-bearing carbonate deposits with horizontal bedding and developed worm-like structures, locally containing intraclasts, biotritus, and grains, representing open platform deposits.

3. Sample Analysis and Testing

The carbon and oxygen isotope testing was conducted by the Kunming Testing Center of the Ministry of Land and Resources, encompassing both sample preparation and analysis. The testing instrument utilized was the MAT253 stable isotope mass spectrometer. For the carbon and oxygen isotope analysis of carbonate rocks, the phosphoric acid

method was employed. Carbonate rock samples underwent a constant-temperature reaction with 100% phosphoric acid under vacuum conditions (limestone at 25 °C for 16 hours; dolomite at 50 °C for 36 hours). Subsequently, carbon dioxide was collected and purified before being analyzed for its carbon and oxygen isotope composition using the MAT253 stable isotope mass spectrometer. The results were calibrated to $\delta^{13}\text{C}$ and $\delta^{18}\text{O}$ values relative to the international standard material (PDB), with GBW-04405 serving as the reference standard. The precision of the test results was $\pm 0.2\%$. In this study, 46 samples from the selected profile were chosen to determine the $\delta^{13}\text{C}$ and $\delta^{18}\text{O}$ values of dolomite and calcite minerals. The collected samples were fresh, unaffected by later metamorphism or alteration, and care was taken to avoid sampling carbonate veins such as calcite to ensure the accuracy of the test results. Ultimately, 34 samples yielded insufficient carbon dioxide gas during the reaction due to low carbonate mineral content, rendering it impossible for the instrument to analyze valid data and resulting in substandard outcomes. The final test results are presented in **Table 1**.

Table 1. Carbon and oxygen isotopic compositions of the Triassic-Permian strata and paleotemperature and paleosalinity of the Yueliangtian section in Xuanwei, northeastern Yunnan Province.

Strata	Sample	Lithological Description	$\delta^{13}\text{C}$ PDB(‰)	$\delta^{18}\text{O}$ PDB(‰)	Delta $\delta^{18}\text{O}$ w.r.t. SMOW SMOW Converted	Sea Temperature T/°C	Ocean Salinity Z
Jialingjiang Formation (T _{1j})	TW46	Limestone	-1.54	-9.30	21.27	17	120
	TW45	Microcrystalline limestone	-3.94	-9.38	21.19	17	115
	TW44	Fine-crystalline limestone	-3.05	-7.79	22.83	11	117
Feixianguan Formation (T _{1f})	TW43	Grainy limestone	-4.24	-9.10	21.48	16	114
	TW42	Dolomitic limestone	-5.62	-8.86	21.72	15	111
	TW41	Limestone	-9.66	-10.20	20.34	21	102
	TW40	Limestone	-1.74	-9.33	21.25	17	119
Xuanwei Formation (P _{3x})	TW23	Thin limestone interlayer	2.05	-8.64	21.23	23	121
	TW16	Thin limestone interlayer	2.68	-8.89	20.18	26	121
the Third Member of the Yangxin Formation (P _{2y} ³)	TW5	Limestone	0.82	-12.20	18.29	31	123
	TW4	Fine-crystalline limestone	-1.72	-11.46	19.05	27	118
	TW3	Limestone	-1.33	-11.72	18.78	28	119
	TW2	Limestone	0.28	-10.20	20.34	21	123
	TW1	Micrite limestone	-2.38	-10.89	19.64	24	117

Notes: The results of carbon and oxygen isotope analysis are derived from the data obtained from this study's analysis; $Z = 2.048 \times (\delta^{13}\text{C} + 50) + 0.498 \times (\delta^{18}\text{O} + 50)$,^[30]; $T^{\circ} = 15.976 - 4.2 \times \delta^{18}\text{O}_{\text{ocaco}_3} + 0.13 \times (\delta^{18}\text{O}_{\text{ocaco}_3} + 0.22)^2$, Among them, $\delta^{18}\text{O}_{\text{ocaco}_3}$ should be calibrated using the average $\delta^{18}\text{O}$ value of Quaternary marine carbonates^[31-33].

4. Analysis Results

4.1. Data Reliability Analysis

It is widely accepted that the carbon and oxygen isotope characteristics of seawater can reflect abundant information about climate, environment, and biological productivity in the ocean during the same period, which is often preserved in intact carbonate sediments. Studies have suggested that

a low water-rock ratio results in minimal changes in carbon isotopes during diagenetic evolution, and that bulk rock oxygen isotopes are in excellent agreement with well-preserved brachiopod shell oxygen isotopes (**Figure 2**). Bulk rock carbon and oxygen isotope curves can thus provide a good reconstruction of the ancient marine environment^[34, 35]. Currently, there is no highly effective method to test the impact of diagenesis on carbonate stable isotopes, but relative judg-

ments can be made with reference to certain thresholds. For example, oxygen isotope thresholds and the correlation between carbon and oxygen isotopes can indirectly reflect the extent of diagenetic effects. When $-11‰ < \delta^{18}\text{O} < -5‰$, the sample has undergone some alteration, but its value can still represent the original sedimentary carbon and oxygen isotope composition; when $\delta^{18}\text{O}$ is significantly less than $-11‰$, the sample may be severely altered, and the carbon and oxygen isotopes can no longer accurately reflect ancient ocean information. Additionally, the correlation between carbon and oxygen isotopes can also indicate the extent to which the sample has undergone diagenetic alteration [36]. In this study, the carbon and oxygen isotope variation ranges of

the Permian-Triassic Boundary (PTB) samples from Haidai, Xuanwei, were $0.82‰$ to $-9.66‰$ and $-12.20‰$ to $-7.79‰$, respectively, with mean values of $-2.84‰$ and $-10.03‰$. All samples had $\delta^{18}\text{O}$ values mostly greater than $-11‰$, except for sample TW5, which had a $\delta^{18}\text{O}$ value of $-12.20‰$, slightly less than $-11‰$. The scatter plot of carbon and oxygen isotopes showed no clear linear relationship and no significant correlation (Figure 3). Overall, this indicates that the isotope composition of the samples was minimally affected by post-diagenetic processes, and the data are reliable, allowing for a relative reflection of the ancient ocean information they carry.

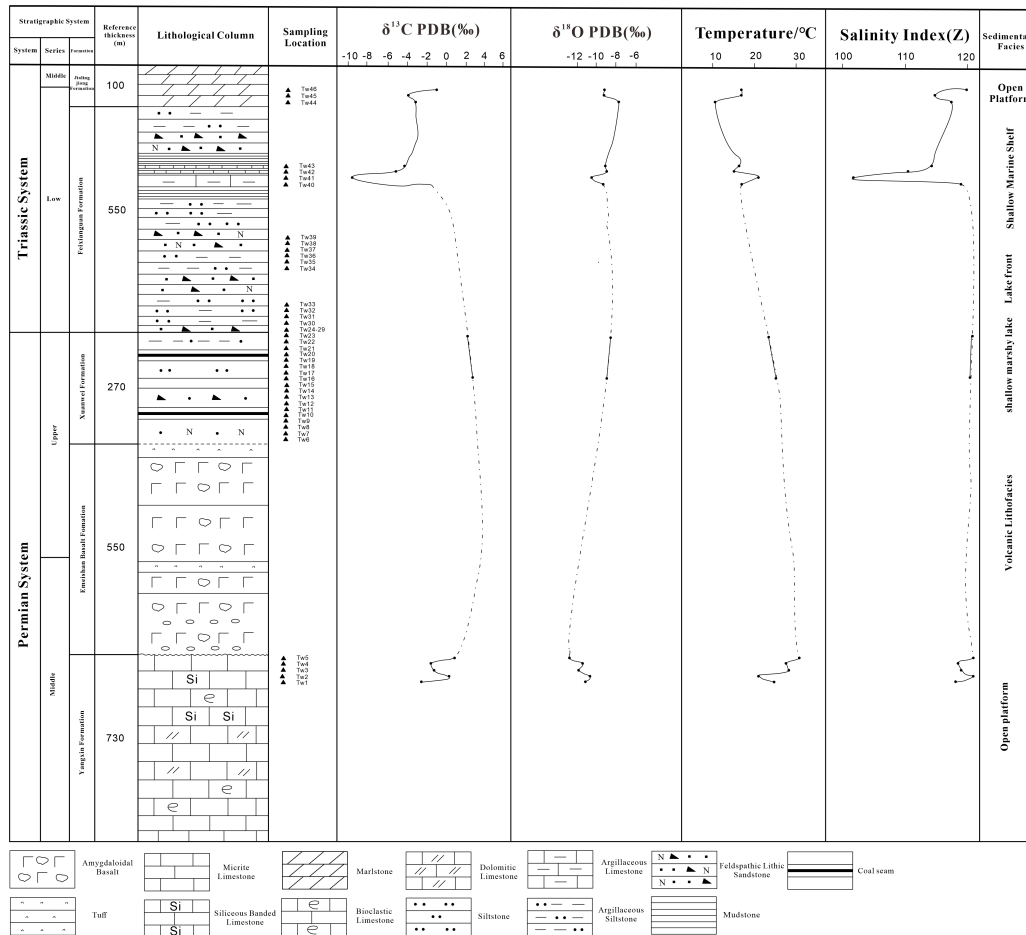


Figure 2. Carbon and oxygen isotope content and paleoenvironmental characteristics of the stratigraphic profile in the study area.

4.2. Carbon Isotope

Similar to the previous description, the carbon isotope at the Haidai PTB section in Xuanwei also exhibits a negative excursion at the boundary. Although carbon isotope data for

the Upper Permian Xuanwei Formation were not obtained, studies have shown that the carbon isotope variation characteristics of this formation are consistent with the analysis presented in this paper [37]. The pattern of carbon isotope variation is as follows: the carbon isotope values in the Mid-

dle Permian Yangxin Formation are overall higher, with a peak around 0.82‰; however, near the boundary, they fluctuate and decrease rapidly to -1.74‰, reaching a minimum of -9.66‰ in the Lower Triassic Feixianguan Formation, and then gradually increase slowly. In summary, there is a clear negative excursion of carbon isotopes at the PTB section, but the change is gradual (**Figure 2**).

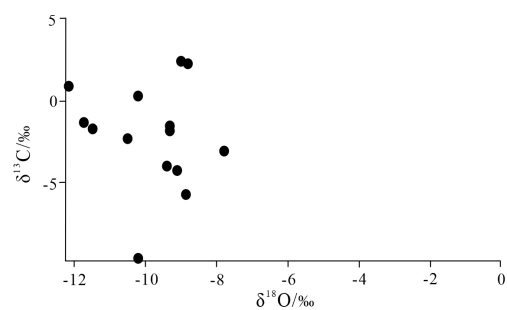


Figure 3. Scatter plot of carbon and oxygen isotopes in the Haidai PTB profile sample in Xuanwei area.

Note: $R^2 = 0.085$; $P = 0.772$.

4.3. Oxygen Isotope

The variation range of oxygen isotopes at the Haidai PTB section in Xuanwei shows a significant negative excursion of oxygen isotopes near the boundary, from -10.20‰ to -12.20‰, with an overall decreasing trend. Subsequently, after entering the Lower Triassic Feixianguan Formation, the oxygen isotopes gradually fluctuate and increase, with a large variation range (-10.20‰ to -7.79‰), and then maintain slight fluctuations.

4.4. Ancient Salinity

The Z value calculated from carbon and oxygen isotope values is often used to indicate the ancient ocean salinity during the same period. Although the Z value is not an absolute value, it has a positive correlation with ancient ocean salinity. Keith proposed a formula for calculating ancient salinity:

$$Z = 2.048 \times (\delta^{13}\text{C} + 50) + 0.498 \times (\delta^{18}\text{O} + 50) \quad (1)$$

When $Z > 120$, it indicates marine limestone; when $Z < 120$, it indicates freshwater limestone, indicating a desalination of seawater. This formula has been widely used to calculate the ancient salinity of pre-Jurassic limestone^[38]. The calculated Z values are shown in **Table 1**. The Middle Permian Yangxin Formation is generally normal marine carbonate rocks. Near the PTB boundary, the salinity decreases

significantly, indicating desalination of seawater. After entering the Lower Triassic Feixianguan Formation, the seawater salinity gradually returns to normal levels.

4.5. Ancient Temperature

The representativeness of the oxygen isotope composition at the Haidai section in Xuanwei for seawater information still needs further evaluation, which is a very difficult issue to discuss. Although estimating ocean temperature based on carbonate isotopes does not have absolute significance, its trend certainly reveals the evolution of seawater. Water temperature is one of the important factors controlling the stable isotope composition of carbonate rocks^[39]. Temperature has a large impact on $\delta^{18}\text{O}$ values but has little impact on $\delta^{13}\text{C}$ values. Therefore, $\delta^{18}\text{O}$ values can be used to effectively determine ancient seawater temperature. The empirical formula is:

$$t^{\circ} = 15.976 - 4.2 \times \delta^{18}\text{O}_{\text{caco}_3} + 0.13 \times (\delta^{18}\text{O}_{\text{caco}_3} + 0.22)^2 \quad (2)$$

Direct application of this formula results in large deviations, which may be due to isotopic age effects, deviations in seawater salinity, and unknown $\delta^{18}\text{O}$ values of seawater at that time. Therefore, samples with normal salinity and $\delta^{18}\text{O}$ values are selected for correction^[40]. Typically, age correction is based on the average $\delta^{18}\text{O}$ value of Quaternary marine carbonates, which is -1.2‰. In this study, the average $\delta^{18}\text{O}$ value of valid samples was -10.0‰, with a difference of 8.8‰ compared to the Quaternary standard. Therefore, $\Delta = 8.8‰$ is used to correct the $\delta^{18}\text{O}$ values of valid samples to make them equivalent to the $\delta^{18}\text{O}$ values of Quaternary samples. Equation (2) was applied to all samples to calculate the ancient seawater temperature during the deposition period (**Table 1**). At the beginning of the Middle Permian Yangxin Formation in the section, the seawater temperature maintained small fluctuations around 25 °C. As it transitioned near the boundary, the ancient seawater temperature fluctuated violently and rose sharply to 32 °C, with temperature fluctuations exceeding 10 °C. Upon entering the Early Triassic, there was a significant drop in temperature, fluctuating near 17 °C, with a temperature drop exceeding 15 °C. Afterward, it maintained a trend of slow temperature increase with fluctuations at lower temperatures.

5. Discussion

Carbon isotope anomalies are often used as auxiliary markers for stratigraphic boundary division and regional correlation of carbonate rocks. The negative excursion of carbon isotopes near the Permian-Triassic Boundary (PTB) not only occurs in South China but is also prevalent in other regions worldwide. In addition, this negative excursion of carbon isotopes, accompanied by mass extinctions, is also observed at the Precambrian-Cambrian boundary and the Cretaceous-Tertiary boundary^[41, 42]. Carbon isotope stratigraphy has played a crucial role in the global stratigraphic division and correlation of the Ediacaran-Cambrian periods^[43–45]; furthermore, studies on the PTB have also employed carbon isotopes as a means for event stratigraphic correlation. This study reveals that the carbon isotopes at the Haidai section in Xuanwei exhibit a pronounced negative excursion at the PTB, with an amplitude close to 9‰, which is very rare and records a significant mass extinction event. Certainly, some current research suggests that there are multiple reasons for the negative excursions of inorganic carbon isotopes during geological history. Besides significant declines in biological productivity or mass extinctions, other factors include volcanic eruptions releasing CO₂ and methane, leading to negative excursions in δ¹³C_{carb}, as well as rapid oxidation of organic carbon reservoirs (such as ancient oil fields or coal seams)^[46]. The profile studied in this research may be the result of the combined effects of mass extinctions and volcanic eruptions on the atmosphere. Along with the gradual negative excursion of carbon isotopes, there are obvious fluctuations in oxygen isotopes at the section. The negative excursion of oxygen isotopes corresponds to fluctuations in sea surface temperatures, with amplitudes approaching 15°, although there is still considerable controversy regarding the estimation of ancient sea surface temperatures, which may involve biases and disagreements over different calculation methods, relatively drastic fluctuations in sea temperatures represent fatal changes for marine biocommunities. Meanwhile, the desalination of seawater poses a challenge to marine biota as well. Compared with the Permian-Triassic boundary section in Meishan^[46], Zhejiang, China, the inorganic carbon isotopes exhibit a notable negative excursion with consistent characteristics, and the variation range of carbon isotopes in this study is even greater. The variation characteristics of oxygen isotopes also show consistency. However, due to the

difference in research precision between this study and the Meishan section, a more detailed layer-by-layer comparison cannot be conducted. Whether it is the Permian-Triassic boundary section in Meishan, Zhejiang or the section studied in this research, the variation characteristics of carbon and oxygen isotopes not only reflect changes in marine productivity but also reveal the coincidence between biological extinction and environmental abrupt changes. By studying different geographical regions, we can better understand the Earth system processes during large-scale biological extinction events. The geological section selected for this study is located in the Emeishan Basalt distribution area, prompting some scholars to question whether the Emeishan Basalt could affect the collected carbonate carbon and oxygen isotope data, thus leading to biased results. The answer to this concern is no. The objects of this research work are carbonate rocks formed by sedimentary processes in a depositional environment, rather than similar calcite veins formed by other means (which can be formed by various causes, such as hydrothermal activity). Only by collecting carbonate rocks formed under normal depositional conditions can their carbonate minerals, such as calcite and dolomite, be considered to have derived their CO₃²⁻ from the atmospheric cycle at that time. These minerals can thus represent the carbon and oxygen isotope composition in the atmosphere and record the results of carbon and oxygen isotope fractionation. If, by accident, samples of carbonate rocks or materials containing calcite and dolomite formed under abnormal depositional conditions, such as calcite veins, are collected, the carbon and oxygen isotopes in the analysis results did not participate in the atmospheric cycle. Their isotope fractionation results are not caused by biological processes but rather by other formation processes. For example, the carbon and oxygen isotope characteristics of calcite derived from magma-hydrothermal processes can reflect geological background features such as the magma source region, and are unrelated to biological processes. Based on the current research approach, using carbon and oxygen isotopes from sediments inherently involves a time lag. After a mass extinction event, it leads to fluctuations in carbon fractionation in the atmosphere. Subsequently, the atmosphere exchanges gases with the ocean, and the fractionated CO₂ eventually enters carbonate rocks and is preserved through deposition. Therefore, the timing of major mass extinction events should precede the formation of car-

bonate rocks in the depositional environment. Consequently, in this study, the observed negative excursion anomaly in the carbon isotope curve that is closer to the Early Triassic is attributed to this cause. Similar situations should also arise in other similar studies worldwide. Overall, near the PTB, sea surface temperatures exhibited significant fluctuations, initially rising sharply and then rapidly decreasing. The seawater showed marked desalination. These characteristics are direct causes of marine and other biological extinctions. However, the trigger for these significant changes in the marine environment and climate has not yet been revealed; the triggers causing drastic oscillations in the marine environment remain unclear.

6. Conclusions

- The carbon isotope profile exhibits a distinct negative excursion mutation at the Permian-Triassic Boundary (PTB). The magnitude of the negative excursion is nearly 9‰. The pattern of carbon isotope variation is as follows: the carbon isotopes in the Middle Permian Yangxin Formation are generally high, with peak values around 0.82‰, but they begin to fluctuate and decrease near the boundary to -1.74‰. The Lower Triassic Feixianguan Formation reaches a nadir of -9.66‰ before gradually increasing, documenting a significant mass extinction event;
- Seawater temperatures in the Middle Permian Yangxin Formation initially fluctuated slightly around 25 °C. As the boundary is approached, ancient seawater temperatures oscillated vigorously and rose sharply to 32 °C, with a temperature fluctuation amplitude exceeding 10 °C. Upon entering the Early Triassic, temperatures began to drop significantly, fluctuating near 17 °C, with a cooling amplitude of over 15 °C. Subsequently, temperatures remained low but gradually increased, indicating drastic fluctuations in the marine environment;
- The Middle Permian Yangxin Formation is generally composed of normal marine carbonate rocks. Near the PTB, salinity decreased significantly, indicating desalination of seawater. After the Lower Triassic Feixianguan Formation, seawater salinity gradually returned to normal levels. The drastic oscillations

in ancient seawater temperature and the apparent desalination near the PTB are direct causes of marine extinctions. However, the trigger for these significant changes in the marine environment and climate has not yet been revealed; the triggers causing drastic oscillations in the marine environment remain unclear.

Author Contributions

Conceptualization, C.L.; methodology, C.L.; validation, C.L. and D.Y.; formal analysis, C.L.; investigation, C.L.; resources, C.L.; data curation, C.L.; writing—original draft preparation, C.L.; writing—review and editing, C.L.; visualization, C.L.; supervision, C.L.; project administration, D.Y.; funding acquisition, D.Y. All authors have read and agreed to the published version of the manuscript.

Funding

This work was supported by the Scientific Research Fund of the Education Department of Yunnan Province (Grant Number: 2019J0488).

Institutional Review Board Statement

Not applicable.

Informed Consent Statement

Not applicable.

Data Availability Statement

All data related to this research project belong to my university. Reasonable access to and consultation of the data for scientific research purposes are permitted. The data published in the paper are authentic experimental data and may be cited.

Conflicts of Interest

The authors declare no conflict of interest.

References

- [1] Benton, M.J., Twitchett, R.J., 2003. How to kill (almost) all life: The end-Permian extinction event.

- Trends in Ecology & Evolution. 18(7), 358–365. DOI: [https://doi.org/10.1016/S0169-5347\(03\)00093-4](https://doi.org/10.1016/S0169-5347(03)00093-4)
- [2] Erwin, D.H., 1994. The Permo-Triassic extinction. *Nature*. 367, 231–236.
- [3] Erwin, D.H., Bowring, S.A., Jin, Y., 2002. End-Permian mass extinctions: A review. *Special Paper of the Geological Society of America*. 356, 363–383.
- [4] Rong, J., Huang, B., 2023. The first brachiopod fauna after the late Ordovician mass extinction: Evidence from silicified brachiopods at the top of the Ordovician in Zhenxiong, Northeastern Yunnan. *Acta Palaeontologica Sinica*. 62(01), 1–29. DOI: <https://doi.org/10.19800/j.cnki.aps.2022036>
- [5] Payne, J.L., Lehrmann, D.J., Wei, J., et al., 2004. Large perturbations of the carbon cycle during recovery from the end-Permian extinction. *Science*. 305, 506–509.
- [6] Huang, E., 1994. Carbon isotope composition of marine carbonate rocks of the Permian-Triassic boundary at Shangchangzi and biological extinction events. *Geochimica*. 23(1), 60–68.
- [7] Zhou, S., Huang, H., Shi, X., et al., 2008. Stable isotope records and major events in environmental and life evolution. *Geological Review*. 54(2), 225–231.
- [8] Cao, C., Wang, W., Jin, Y., 2002. Carbon isotope variations near the Permian/Triassic boundary at Meishan, Zhejiang Province. *Chinese Science Bulletin*. 47(4), 302–305.
- [9] Xie, S., Pancost, R.D., Huang, J., et al., 2007. Changes in the global carbon cycle occurred as two episodes during the Permian-Triassic crisis. *Geology*. 35(12), 1083–1086.
- [10] Joachimski, M.M., Lai, X., Shen, S., et al., 2012. Climate warming in the latest Permian and the Permian-Triassic mass extinction. *Geology*. 40(3), 195–198. DOI: <https://doi.org/10.1130/G32707.1>
- [11] Zhang, W., 1991. New progress in isotope geological science and technology. *Geological Science and Technology Information*. 10(2), 67–72.
- [12] Li, R., Lu, J., Zhang, S., et al., 1999. Organic carbon isotope composition of black shales from the Sinian and Early Cambrian. *Science in China: Series D*. 29(4), 351–357.
- [13] Teng, G., Liu, W., Xu, Y., et al., 2004. Identification of effective source rocks in Ordovician marine deposits, Ordos Basin. *Progress in Natural Science*. 14(11), 1249–1256.
- [14] Gao, Z., Fan, T., Jiao, Z., et al., 2006. Carbonate platform styles and sedimentary response characteristics of the Cambrian-Ordovician in the Tarim Basin. *Acta Sedimentologica Sinica*. 24(1), 19–27.
- [15] Liu, D., Sun, X., Li, Z., et al., 2006. Carbon and oxygen isotope analysis of Ordovician dolomite in the Ordos Basin. *Petroleum Geology & Experiment*. 28(2), 155–161.
- [16] Wang, K., Li, W., Lu, J., et al., 2011. Carbon, oxygen, and strontium isotope characteristics of Carboniferous carbonate rocks in eastern Sichuan and their genetic analysis. *Geochimica*. 40(4), 351–362.
- [17] Chen, Q., Zhang, H., Li, W., et al., 2012. Carbon and oxygen isotope characteristics of Ordovician carbonate rocks in the Ordos Basin and their significance. *Journal of Palaeogeography*. 14(1), 117–124.
- [18] Huang, S., Li, X., Hu, Z., et al., 2016. Comparison of carbon and oxygen isotope compositions of Triassic Feixianguan Formation carbonate rocks on both sides of the Kaijiang-Liangping trough in eastern Sichuan Basin and its palaeoceanographic significance. *Geochimica*. 45(1), 24–40.
- [19] Shen, S., Cao, C., Zhang, H., et al., 2019. High-resolution $\delta^{13}\text{C}$ records and phased extinction patterns at the Permian-Triassic boundary. *Earth-Science Reviews*. 189, 244–259.
- [20] Song, X.Y., Chen, L.M., Deng, Y.F., et al., 2013. Syn-collisional tholeiitic magmatism induced by asthenosphere upwelling due to slab detachment at the southern margin of the Central Asian Orogenic Belt. *Journal of the Geological Society*. 170(6), 941–950. DOI: <https://doi.org/10.1144/jgs2012-049>
- [21] Stanley, S.M., 1988. Paleozoic mass extinctions: shared patterns suggest global cooling as a common cause. *American Journal of Science*. 288, 334–352.
- [22] Kozur, H.W., 1998. Some aspects of the Permian Triassic boundary (PTB) and of the possible causes for the biotic crisis around this boundary. *Palaeogeography, Palaeoclimatology, Palaeoecology*. 143, 227–272.
- [23] Jin, Y., Wang, Y., Wang, W., et al., 2002. Pattern of marine mass extinction near the Permian-Triassic boundary in South China. *Science*. 289, 432–436.
- [24] Holser, W.T., Schonlaub, H.P., Attrep, J.M., et al., 1989. A unique geochemical record at the Permian/Triassic boundary. *Nature*. 337, 39–44.
- [25] Korte, C., Kozur, H.W., Bachmann, G.H., 2007. Carbon isotope values of Triassic lacustrine and hypersaline playa lake carbonates: lower Buntsandstein and middle Keuper (Germany). *Hallesches Jahrbuch für Geowissenschaften*. 29, 1–10.
- [26] Korte, C., Kozur, H.W., Mohtat Aghai, P., 2004. Dzhulfian to lowermost Triassic $\delta^{13}\text{C}$ record at the Permian/Triassic boundary section at Shahreza, Central Iran. *Hallesches Jahrbuch für Geowissenschaften B Beiheft*. 18, 73–78.
- [27] Horacek, M., Brandner, R., Abaet, R., 2007. Carbon isotope of the P-T boundary and the Lower Triass in the Southern Alps: Evidence for rapid changes in storage of organic carbon. *Palaeogeography, Palaeoclimatology, Palaeoecology*. 252, 347–354.
- [28] Zhang, X., Hu, X., Li, J., et al., 2024. Sedimentological and carbon isotope records of the carbonate platform mortality event at the end of the Early Permian in the Lower Yangtze Region. *Geological*

- Journal of China Universities. 30(04), 379–396. DOI: <https://doi.org/10.16108/j.issn1006-7493.2023030>
- [29] Wang, J., 2015. Geochemical Characteristics and Paleoenvironmental Implications of the P/T Boundary Coals in Xuanwei, Yunnan [PhD thesis]. Beijing, China: China University of Mining and Technology. pp. 41–42.
- [30] Shao, L., Dou, J., Zhang, P., 1996. The paleogeographic significance of oxygen and carbon stable isotopes in the Late Permian of southwestern China. *Geochimica*. 25(6), 575–581.
- [31] Kaufman, A.J, Knoll, A.H., 1995. Neoproterozoic variations in the C isotope composition of seawater: stratigraphic and biogeochemical implications. *Precambrian Research*. 73(1/2/3/4), 27–49.
- [32] Meng, H., Ren, Y., Zhong, D., et al., 2016. Geochemical characteristics and paleoenvironmental implications of the Cambrian Longwangmiao Formation in eastern Sichuan Basin. *Natural Gas Geoscience*. 27(7), 1299–1311.
- [33] Korte, C., Kozur, H.W., Veizer, J., 2005. $\delta^{13}\text{C}$ and $\delta^{18}\text{O}$ values of Triassic brachiopods and carbonate rocks as proxies for coeval seawater and palaeotemperature. *Palaeogeography, Palaeoecology, Palaeoclimatology*. 226(3/4), 287–306.
- [34] Wynn, T.C., Read, J.F., 2007. Carbon-oxygen isotope signal of Mississippian slope carbonates, Appalachians, USA: A complex response to climate-driven fourth-order glacio-eustasy. *Palaeogeography, Palaeoecology, Palaeoclimatology*. 256(3/4), 254–272.
- [35] Wang, D., Feng, X., 2002. Geochemical study of carbon and oxygen isotopes in the Lower Paleozoic of the Bohai Bay area. *Acta Geologica Sinica*. 76(3), 400–408.
- [36] Li, Q., Jin, Z., Jiang, F., 2014. Preliminary exploration of carbon and oxygen isotope analysis methods for dolomite genesis: A case study of the Proterozoic dolomite in the Yanshan area of Beijing. *Lithologic Reservoirs*. 26(4), 117–122.
- [37] Keith, M.H., Weber, J.N., 1964. Isotopic composition and environmental classification of selected fossils. *Geochimica et Cosmochimica Acta*. 28, 1787–1816.
- [38] Kong, W., Li, S., Wan, Q., et al., 2011. Carbon and oxygen isotope characteristics and their significance of the Permian in Xikou area, Zhen'an. *Journal of Hefei University of Technology (Natural Science Edition)*. 34(7), 1058–1065.
- [39] Wang, S., Gao, L., Pang, Q., et al., 2015. The terrestrial Jurassic-Cretaceous boundary in China and its international stratigraphic correlation: A case study of the Jurassic-Cretaceous chronostratigraphy in the northern Hebei-western Liaoning area. *Acta Geologica Sinica*. 89(8), 1331–1351.
- [40] Chen, L., Zhong, H., Hu, R., et al., 2006. Early Cambrian anoxic events in northern Guizhou: Characteristics of biomarker compounds and organic carbon isotopes. *Acta Petrologica Sinica*. 22(9), 2413–2423.
- [41] Ishikawa, T., Ueno, Y., Komiya, T., et al., 2008. Carbon isotope chemostratigraphy of a Precambrian-Cambrian boundary section in the Three Gorge area, South China: Prominent global scale isotope excursions just before the Cambrian Explosion. *Gondwana Research*. 14(1–2), 193–208.
- [42] Yuan, Y., Cai, C., Wang, T., et al., 2014. Redox condition during Ediacaran-Cambrian transition in the Lower Yangtze deep water basin, South China: Constraints from iron speciation and $\delta^{13}\text{C}_{\text{org}}$ in the Diben section, Zhejiang. *Chinese Science Bulletin*. 59(23), 3638–3649.
- [43] Haas, J., Demeny, A., Hips, K., et al., 2006. Carbon isotope excursions and microfacies in marine Permian-Triassic sections in Hungary. *Palaeogeography, Palaeoclimatology, Palaeoecology*. 237(2–4), 160–181.
- [44] Luo, G., Huang, J., Xie, S., et al., 2010. Relationships between carbon isotope evolution and variation of microbes during the Permian-Triassic transition at Meishan Section, South China. *International Journal of Earth Sciences*. 99(4), 775–784.
- [45] Song, H., Wignall, P.B., Tong, J., et al., 2012. Geochemical evidence from bioapatite for multiple oceanic anoxic events during Permian-Triassic transition and the link with end-Permian extinction and recovery. *Earth and Planetary Science Letters*. 353(1), 12–21.
- [46] Nan, J., Liu, Y., 2004. Variations of organic and inorganic carbon isotopes and paleoenvironment at the Permian-Triassic boundary section in Meishan, Zhejiang. *Geochimica*. 33(1), 9–19. DOI: <https://doi.org/10.3321/j.issn:0379-1726.2004.01.002>